European Conference on Computational Fluid Dynamics
ECCOMAS CDF 2006
P. Wesseling, E. Oñate, J. Périaux (Eds)
© TU Delft, Delft The Netherland, 2006

THE INFLUENCE OF ASYMMETRIC INFLOW IN ABDOMINAL AORTIC ANEURYSM HEMODYNAMICS

Yannis Papaharilaou[1], John A. Ekaterinaris[1,2] *

[1]Institute of Applied and Computational Mathematics,
Foundation for Research and Technology-Hellas,
Vasilika Vouton, Heraklion, Crete, 71110, Greece
e-mail: yannisp@iacm.forth.gr

[2]Dept. of Mechanical and Aerospace Engineering,
University of Patras, Patra, Rio, 26500, Greece
e-mail: ekaterin@iacm.forth.gr

Key words: Local Hemodynamics, Aneurysm Rupture, Aneurysm Tortuosity

Abstract. *Inflow asymmetry has been found to strongly influence the hemodynamics in arterial geometries. Flow asymmetry is commonly found within the aortic conduit just proximal of the aneurysmal expansion and is caused by the remodeling of the abdominal aorta required to accommodate the excess volume of the distended vessel. In an effort to improve the accuracy of abdominal aortic aneurysm (AAA) rupture risk estimation the influence of parameters other than the peak transverse dimension, used routinely in clinical practice as a rupture risk index, on the distribution of wall stress is investigated. Towards this end, both experimental and computational flow studies in simplified geometry AAA models have been conducted. However, these studies neglect the presence of significant vessel tortuosity of the AAA inflow segment. This paper is primarily concerned with the effects of asymmetric inflow on abdominal aortic aneurysmal sac flow. To assess the influence of inflow asymmetry on the intra-aneurysmal flow features we compare the numerically computed time varying flow fields in two simplified geometry AAA models, one with a straight pipe inflow and another with an s-shaped inflow conduit. The tortuosity of the s-shaped AAA inlet was set to be equal to the mean inflow tortuosity derived from patient specific AAA wall surface models created by 3D reconstruction of in vivo acquired Computed Tomography images. The Womersley solution of a physiologic abdominal aortic flow waveform was used to compute the time varying velocity profile applied as the model inflow boundary condition. Our results show that the injection of an asymmetric velocity profile in the aneurysmal sac affects the distribution of wall stress thus influencing the progression of AAA wall disease and subsequently the risk of rupture.*

1 INTRODUCTION

Abdominal aortic aneurysm is a localized dilatation of the aortic wall. The physiological processes associated with AAA development and progression are not as yet fully understood. This pathologic condition has been found to affect 8.8 % of the population over the age of 65[1]

and if left untreated it may lead to rupture. The size of the aneurysm and its rate of expansion are parameters associated with the risk of rupture. For aneurysms with a maximum transverse diameter below 4 cm the risk of rupture is very small (but not absent). However, when the aneurysm transverse diameter is between 4 and 5 cm the risk of rupture is 0.5 % and between 5 and 6 cm it becomes 5 % rising exponentially with diameter increase [2]. The decision for surgical intervention for patients with an abdominal aortic aneurysm (AAA) is complicated by the lack of a sufficiently accurate rupture risk index. A widely used such index, based on the results from a number of clinical studies [3], is the maximum transverse diameter. In cases where this diameter exceeds 5-6 cm, surgical or endovascular treatment is advised. However 'small' (<5 cm) diameter aneurysms, where 'watchful waiting' requiring frequent observation is preferred to surgery, are known to rupture [4]. Therefore, the decision for surgical intervention, associated with a mortality rate of 4-5 % [5], should not be based exclusively on the maximum transverse diameter and a new more reliable rupture risk index should be introduced.

Recent attempts to establish a reliable AAA rupture risk index were based on the evaluation of the arterial wall stress distribution. Finite element analysis has been used to compute the stress distribution in both simplified [6] and anatomically correct AAA models. The hemodynamics of the AAA have been extensively investigated experimentally [7, 8] and computationally in both idealized and anatomically correct models in steady and time varying flow [9-11]. The coupling of fluid and structure has also been studied in AAA models [12]. However, these studies of aneurysm hemodynamics neglect the presence of significant vessel tortuosity of the AAA inflow segment, a geometric feature strongly correlated to the peak aneurysm transverse dimension.

The stress distribution on the aneurysmal wall is determined by the complex intra-aneurysmal hemodynamics resulting from the geometric configuration of the intraluminal thrombus (ILT) modulated flow conduit and the effects of surrounding tissue. The altered geometric configuration of the aneurysmal aortic bifurcation caused by the directionally constrained expansion of the sac wall creates an s-shaped aneurysm neck section that alters the velocity profile injected in the sac expansion region. The asymmetric velocity profile affects the vortical structures that develop downstream and the transport and mixing of particles such as red blood cells and platelets [13].

The lack of an accurate AAA rupture risk index remains an important problem in the clinical management of the disease. Accurate estimation of the patient specific AAA rupture risk requires detailed information on both the wall stress distribution and the aortic wall tissue yield stress. However, the AAA wall properties and the stress distribution cannot be measured or even derived with sufficient accuracy from non-invasive measurements *in vivo*. Alternatively, numerical approximations of the flow and wall motion equations are sought using wall constitutive models based on mean elastic properties obtained by *in vitro* mechanical testing of excised specimens of the aneurysmal wall. However, the value of the results obtained by this approach strongly depends on the geometry and boundary conditions applied. Towards this end, this study aims to assess the influence of the sac inlet geometry on the intra-aneurysmal flow field. In this work the case of a "small" idealized aneurysm with a planar s-shaped inlet is investigated.

2 MATERIALS AND METHODS

2.1 Computational Domain

The models used in this study can be decomposed into four sections: a) the inlet, b) the aneurysm sac, c) the aortic bifurcation and d) the iliac arteries (Fig. 1). Two simplified AAA model geometries were investigated that only differed only in the inlet section. One had a straight pipe inlet of diameter D and the other a planar s-bend inlet of the same diameter. The plane defined by the s-bend inlet centerline lies normal to the plane defined by the centerlines of the aneurysmal sac and the iliac arteries (Fig. 1). The tortuosity of the s-shaped inlet was defined as $T_o = L/d-1$ where L the arc length of the inlet centerline and d the distance between its end-points. A value of $T_o = 0.02$ was used to create the model inlet based on the mean values of *in vivo* extracted AAA geometries of similar peak transverse dimension. The aneurysmal sac was modeled as a symmetric ellipsoid with a peak normal dimension of 1.8D and a longitudinal dimension of 4D. The abdominal bifurcation was planar and symmetric with a 70 degrees angle. The iliac arteries were modeled as straight tubes of 0.65D diameter and 7D length. The computational grids were generated using Gambit (Fluent Inc.). Non-uniform grid node spacing was applied to produce higher grid density at the aneurysm neck and the distal aneurysm sac regions as compared to the bulge surface. The curved inlet model was symmetric about the xz plane thus only half of the model was spatially discretised using 158877 elements. The straight inlet model was symmetric about both the xz and yz planes thus only ¼ of the geometry was spatially discretised using 85784 elements.

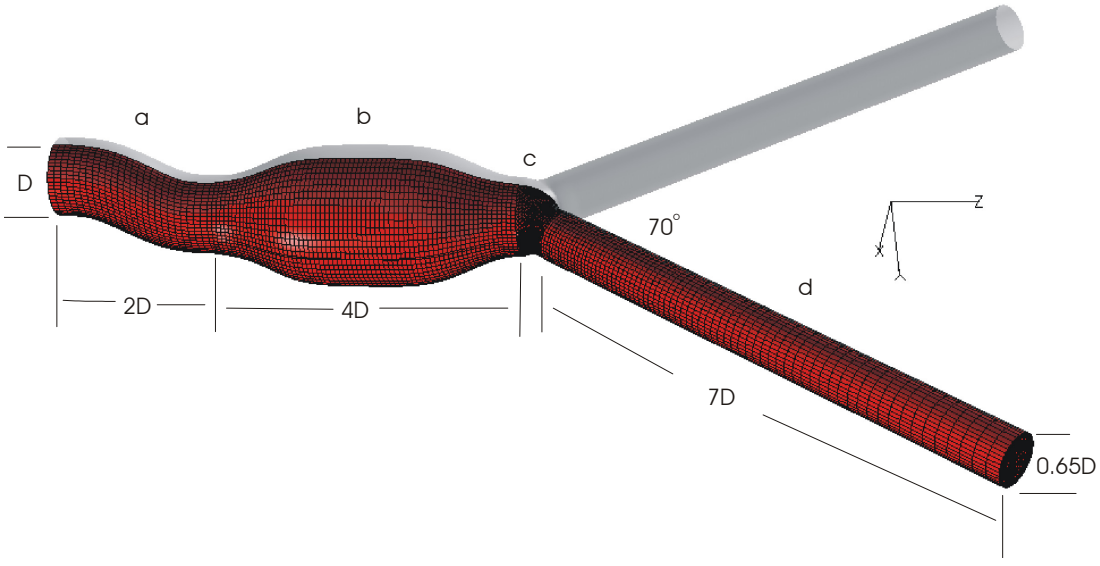

Figure 1: The curved inlet computational domain.

2.2 Flow Computation

The exact Womersley solution was applied at the inlet as the time dependent inflow boundary condition. The Navier-Stokes and continuity equations for incompressible flow neglecting body forces are expressed in vector form as:

$$\nabla \cdot \mathbf{u} = 0$$
$$\frac{D\mathbf{u}}{Dt} = -\frac{1}{\rho}\nabla p + \nu\nabla^2\mathbf{u} \tag{1}$$

where, $D/Dt = \partial/\partial t + \mathbf{u}\cdot\nabla$ is the substantial derivative, ρ is the fluid density, and v is the fluid kinematic viscosity.

Fluent 6.1.22 (Fluent Inc.) was used to solve the flow equations. The arterial wall was assumed rigid and blood was modeled as an incompressible, Newtonian fluid with a density of 1.05 gr/cm^3 and a viscosity of 4.5 cP. Blood is a suspension of red and white cells, platelets, proteins and other elements in plasma and exhibits an anomalous non-Newtonian viscous behavior when exposed to low shear rates or flows in tubes of less than 1mm in diameter. However, the Newtonian fluid assumption does not affect the major flow features and is considered an acceptable approximation for modeling blood flow in the macrocirculation [14] . The inflow waveform used was measured *in vivo* by Doppler US from a patient with an AAA. An equal flow split between left and right iliac arteries was applied. The discrete Fourier series of the measured AAA inflow waveform can be expressed as:

$$Q(t) = Q_0 + \sum_{n=1}^{N} Q_n e^{in\omega t} \tag{2}$$

where Q_0 is the steady flow component, N=16 represents the number of Fourier modes used and ω is the fundamental frequency of the measured flow waveform. From the discrete Fourier series of the volume flow rate in Eq. (2) the fully developed time varying velocity profile was computed using an expression obtained following Womersley's derivation [15] :

$$u(r,t) = \frac{2Q_0}{A}\left(1-\frac{r^2}{R^2}\right) + \sum_{n=1}^{N}\frac{Q_n}{A}\left\{\left(1-\frac{J_0(\alpha_n i^{3/2} r/R)}{J_0(\alpha_n i^{3/2})}\right)/\left(1-\frac{2J_1(\alpha_n i^{3/2})}{\alpha_n i^{3/2} J_0(\alpha_n i^{3/2})}\right)\right\} e^{in\omega t} \tag{3}$$

where J_0 and J_1 are the Bessel functions of the first kind of order zero and one respectively, A is the cross sectional area and R the inlet radius of the straight tube extension inlet and, $\alpha_n = R\sqrt{n\omega/\nu}$ is the Womersley parameter. The time averaged mean Reynolds number of the prescribed waveform was Re_m=355 and the Womersley parameter for the fundamental frequency of the measured flow waveform was α_1=16.7. The velocity profile given by Eq. (3) with time variation of the mean velocity (Q_i / A, $i = 0,..N$) shown in Fig. 2 was applied as the

time dependent inflow boundary condition. A time step size of 3×10^{-4} s was used and 2×10^{4} time steps were required to complete one flow cycle. A time periodic solution was achieved after 5 flow cycles. A second order upwind discretization scheme was applied for the momentum equation and the SIMPLE scheme was used for pressure velocity coupling. A systematic time-step and grid size independence study was carried out to assess the accuracy of the numerical computations. Details of the method used are described elsewhere [16]. Tecplot (Amtec Inc.) was used for flow visualisation.

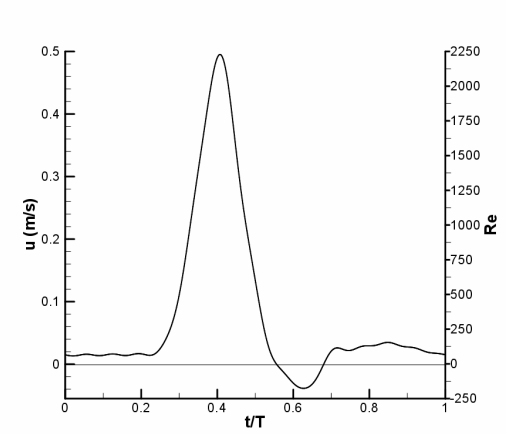

Figure 2: Mean velocity waveform and instantaneous Reynolds number (Re) prescribed at the AAA inlet.

3 RESULTS AND DISCUSSION

3.1 Wall Shear Stress

The injected velocity profile asymmetry in the curved inlet configuration modulates the wall shear distribution in a spatially constrained region that extents up to the proximal end of the aneurysm sac. Wall shear stress within the aneurysmal expansion was generally low throughout the flow cycle except from the proximal and distal end sections which were exposed to higher shearing forces mainly during late systolic acceleration and early systolic deceleration. This was primarily due to the changes in the shape and size of the flow conduit that occurs in these sections. Furthermore, as fluid negotiates the aortic bifurcation swiftly changing bulk direction strong in-plane forces are required that change the local flow field. The asymmetry of the wall shear stress (WSS) distribution in the proximal end of the sac becomes apparent just before peak systolic acceleration t/T=0.375 and is preserved with higher shearing forces on the anterior wall until early systolic deceleration, t/T=0.425 (Fig. 3). Wall shear stress magnitude was normalized by the straight pipe inlet Poiseuille WSS calculated using the mean Reynolds number of the flow waveform. Significant WSS gradients also develop during this phase of the cycle primarily on the anterior wall. This localized asymmetry becomes more significant and its distribution pattern reverses during late systolic deceleration t/T=0.5 (Fig. 3) with the posterior walls near the proximal end of the sac exposed

to higher stresses (peak normalized stress value 28) than the opposite anterior walls (peak normalized stress value 14).

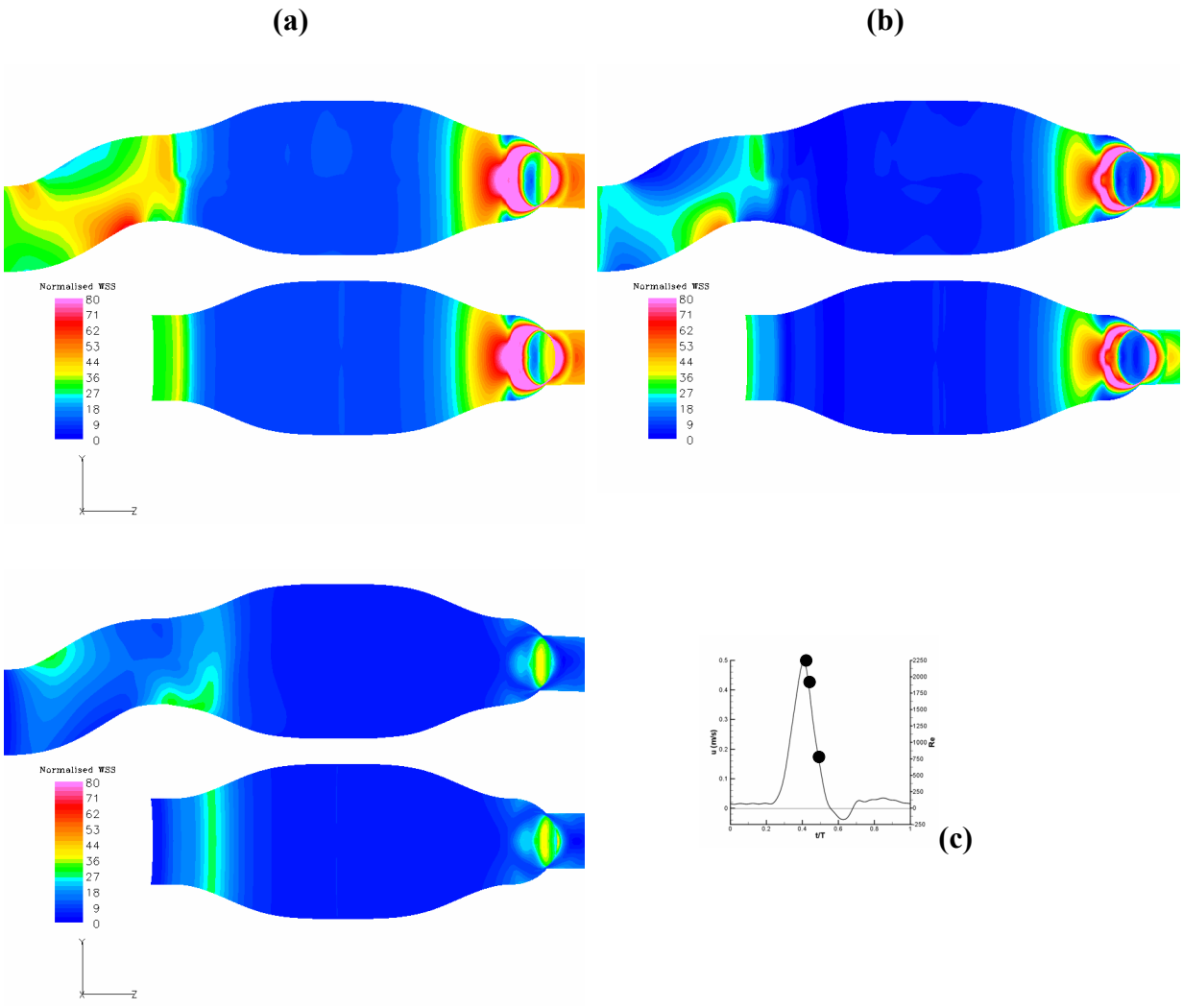

Figure 3: Normalized wall shear distribution during peak systole (a) early systolic deceleration (b) and end systolic deceleration (c).

It is also worth noting the presence of elevated wall shear regions that develop within the proximal section of the curved AAA inlet wall during late systolic acceleration and early systolic deceleration that are absent in the straight inlet case. Platelets exposed to high shear as they flow through the inlet section may become activated and thus ready to attach

downstream in the sac region at wall sites exposed to low shear if they remain close to the wall for sufficient time thus initiating the thrombus formation process. A common finding even in small aneurysms with a 4 cm peak transverse diameter is the presence of intraluminal thrombus ILT which modulates the shape of the aneurysmal flow conduit. The role of ILT in AAA pathogenesis and disease progression has not been fully understood. However, local hemodynamics strongly influence the thrombus formation process by creating favorable conditions such as low shear stress and high shear gradients for activated platelet attachment to the arterial wall. Such flow conditions are commonly associated with flow expansion regions created in aneurysmal arteries where boundary layer separation and recirculation regions develop.

3.2 Hemodynamic Pressure

The normal component of stress is the primary mechanical load on the aneurysmal wall and thus plays a significant role in aneurysm pathophysiology. The distribution of pressure load on the aneurysmal wall in real AAA geometry models has been found [16] to be non-uniform with its peak intra-aneurysmal variation occurring during early systolic deceleration.

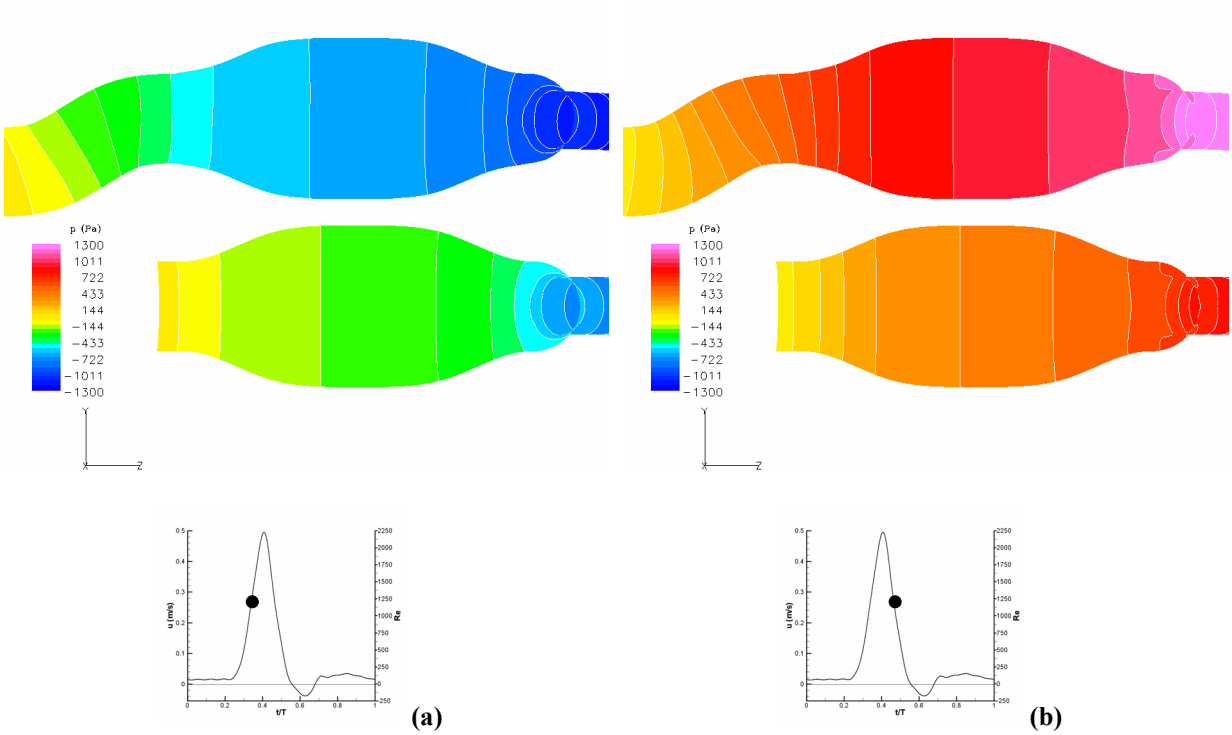

Figure 4: Pressure distribution on AAA wall during mid systolic acceleration t/T=0.35 (a) and mid systolic deceleration t/T=0.45 (b)

In the idealized AAA geometries used in this study significant sac wall pressure variation occurs mainly during the mid systolic acceleration and mid systolic deceleration phases of the

flow cycle (Fig. 4). Peak intra-aneurysmal sac pressure drop for the curved inlet case occurs just after mid-systolic acceleration (t/T=0.35) and was approximately 0.6 kPa. The respective value for the straight pipe inlet was 0.45 kPa. During mid systolic deceleration (t/T=0.45) an intra-aneurysmal sac pressure drop of 0.6 kPa was found in the curved inlet and of 0.5 kPa in the straight inlet model. The site of peak pressure in both cases was located near the distal end of the sac. Inlet curvature in this case does not appear to significantly alter the intra-aneurysmal hemodynamic pressure distribution pattern for the model geometries investigated.

4 CONCLUSIONS

The influence of inlet curvature in a “small” idealized AAA was investigated. Shape and size of the aneurysmal expansion are known to influence the local intra-aneurysmal hemodynamics. The results of this study show that the planar s-shaped AAA inlet geometry configuration influences the aneurysmal sac flow field creating a localized asymmetry in the WSS distribution in the vicinity of the proximal end of the sac and exposing regions of the inlet wall to relatively high shear stress as compared to the straight inlet case. Only minor differences in intra-aneurysmal hemodynamic pressure distribution were found between the straight and curved inlet AAA models. However, the influence of inlet geometry is related to the degree of inlet tortuosity which is in turn strongly correlated to peak transverse sac dimension. Thus further flow investigations in a range of aneurysm models are required to establish the association between aneurysm size, inlet tortuosity and intra-aneurysmal hemodynamics.

REFERENCES

[1] A. B. Newman, A. M. Arnold, G. L. Burke, D. H. O'Leary, and T. A. Manolio, "Cardiovascular disease and mortality in older adults with small abdominal aortic aneurysms detected by ultrasonography: the cardiovascular health study", *Ann Intern Med*, 134, 182-90, (2001).

[2] Y. G. Wolf and E. F. Bernstein, "A current perspective on the natural history of abdominal aortic aneurysms", *Cardiovasc Surg*, 2, 16-22, (1994).

[3] R. A. Scott, H. A. Ashton, and M. J. Lamparelli, "Vascular surgical society of great britain and ireland: fifteen years of experience using 6 cm as a criterion for abdominal aortic aneurysm surgery", *Br J Surg*, 86, 709-10, (1999).

[4] S. C. Nicholls, J. B. Gardner, M. H. Meissner, and H. K. Johansen, "Rupture in small abdominal aortic aneurysms", *J Vasc Surg*, 28, 884-8, (1998).

[5] D. A. Katz, B. Littenberg, and J. L. Cronenwett, "Management of small abdominal aortic aneurysms. Early surgery vs watchful waiting", *Jama*, 268, 2678-86, (1992).

[6] D. F. Elger, D. M. Blackketter, R. S. Budwig, and K. H. Johansen, "The influence of shape on the stresses in model abdominal aortic aneurysms", *J Biomech Eng*, 118, 326-32, (1996).

[7] C. J. Egelhoff, R. S. Budwig, D. F. Elger, T. A. Khraishi, and K. H. Johansen, "Model studies of the flow in abdominal aortic aneurysms during resting and exercise conditions", *J Biomech*, 32, 1319-29, (1999).

[8] S. C. M. Yu, "Steady and pulsatile flow studies in Abdominal Aortic Aneurysm models using Particle Image Velocimetry", *International Journal of Heat and Fluid Flow*, 21, 74-83, (2000).

[9] R. Budwig, D. Elger, H. Hooper, and J. Slippy, "Steady flow in abdominal aortic aneurysm models", *J Biomech Eng*, 115, 418-23, (1993).

[10] T. W. Taylor and T. Yamaguchi, "Three-dimensional simulation of blood flow in an abdominal aortic aneurysm--steady and unsteady flow cases", *J Biomech Eng*, 116, 89-97, (1994).

[11] E. A. Finol, K. Keyhani, and C. H. Amon, "The effect of asymmetry in abdominal aortic aneurysms under physiologically realistic pulsatile flow conditions", *J Biomech Eng*, 125, 207-17, (2003).

[12] E. S. Di Martino, Guadagni, G., Fumero A., Ballerini G., Spirito, and B. P. R., Redaelli, A., "Fluid-structure interaction within realistic three-dimensional models of the aneurysmatic aorta as a guidance to assess the risk of rapture of the aneurysm", *Medical Engineering and Physics*, 23, 647-655, (2001).

[13] D. J. Doorly, S. J. Sherwin, P. T. Franke, and J. Peiro, "Vortical flow structure identification and flow transport in arteries", *Comput Methods Biomech Biomed Engin*, 5, 261-73, (2002).

[14] K. Perktold, M. Resch, and H. Florian, "Pulsatile non-Newtonian flow characteristics in a three-dimensional human carotid bifurcation model", *J Biomech Eng*, 113, 464-75, (1991).

[15] J. R. Womersley, "Method for the calculation of velocity, rate of flow and viscous drag in arteries when the pressure gradient is known", *J Physiol*, 127, 553-63, (1955).

[16] Y. Papaharilaou, J. A. Ekaterinaris, E. Manousaki, and A. N. Katsamouris, "A decoupled fluid structure approach for estimating wall stress in abdominal aortic aneurysms", *J Biomech*, (2006).